

Article

Biochars as Potential Adsorbers of CH₄, CO₂ and H₂S

Sumathi Sethupathi ¹, Ming Zhang ², Anushka Upamali Rajapaksha ^{3,4}, Sang Ryong Lee ⁵, Norhusna Mohamad Nor ⁶, Abdul Rahman Mohamed ⁶, Mohammad Al-Wabel ⁷, Sang Soo Lee ^{3,*} and Yong Sik Ok ^{3,*}

¹ Faculty of Engineering and Green Technology, Universiti Tunku Abdul Rahman, 31900 Kampar, Perak, Malaysia; sumathi@utar.edu.my

² Department of Environmental Engineering, China Jiliang University, Hangzhou 310018, China; m.zhang.env@163.com

³ Korea Biochar Research Center & School of Natural Resources and Environmental Science, Kangwon National University, Chuncheon 24341, Korea; anushkaupamali@gmail.com

⁴ Department of Basic Sciences, Faculty of Health Sciences, The Open University of Sri Lanka, Nawala, Nugegoda 10250, Sri Lanka

⁵ National Institute of Animal Science, RDA, Wanju55365, Korea; soilsang@gmail.com

⁶ School of Chemical Engineering, Universiti Sains Malaysia, 14300 Nibong Tebal, Pulau Pinang, Malaysia; uena86@gmail.com (N.M.N.); chrahman@usm.my (A.R.M.)

⁷ Soil Science Department, College of Food & Agricultural Sciences, King Saud University, P.O. Box 2460, Riyadh 11451, Saudi Arabia; malwabel@lova-serv.com

* Correspondence: sslee97@kangwon.ac.kr (S.S.L.); soilok@kangwon.ac.kr (Y.S.O.); Tel.: +82-33-250-7214 (S.S.L.); +82-33-250-6443 (Y.S.O.); Fax: +82-33-241-6640 (S.S.L. & Y.S.O.)

Academic Editor: Marc A. Rosen

Received: 10 November 2016; Accepted: 4 January 2017; Published: 14 January 2017

Abstract: Methane gas, as one of the major biogases, is a potential source of renewable energy for power production. Biochar can be readily used to purify biogas contaminants such as H₂S and CO₂. This study assessed the adsorption of CH₄, H₂S, and CO₂ onto four different types of biochars. The adsorption dynamics of biochars were investigated in a fixed-bed column, by determining the breakthrough curves and adsorption capacities of biochars. The physicochemical properties of biochars were considered to justify the adsorption performance. The results showed that CH₄ was not adsorbed well by the subjected biochars whereas CO₂ and H₂S were successfully captured. The H₂S and CO₂ breakthrough capacity were related to both the surface adsorption and chemical reaction. The adsorption capacity was in the following order: perilla > soybean stover > Korean oak > Japanese oak biochars. The simultaneous adsorption also leads to a competition of sorption sites. Biochars are a promising material for the biogas purification industry.

Keywords: adsorption; biochar; carbon dioxide; hydrogen sulphide

1. Introduction

Biogas has been identified as one of the prominent renewable energy sources worldwide. Biogases are mainly produced in digesters of anaerobic processes in industries, landfills, and domestic wastes. The palm oil industry is one of the potential large producers of biogas. Palm oil mill effluent (POME) can be degraded in an anaerobic digester to produce biogas. A 30 t fresh fruit bunch per hour produces POME which can generate methane with a yearly burning rate of 12.0 million liters of fuel oil [1,2]. The POME biogas upgrading process is expensive and contains impurities, and the captured biogas is usually flared in palm oil mills. It is suggested that a new economic method should be introduced to extract POME biogas energy with some primary pretreatments such as using adsorbents [3].

The current concern about the harvesting of biogas energy from POME is its enrichment of methane and the removal of impurities such as hydrogen sulphide (H₂S) and carbon dioxide (CO₂). The removal of H₂S as one of the major impurities is particularly crucial to avoid facility corrosion, unnecessary byproducts, and possible public exposure and complaints [4]. Many studies have introduced the generic removal methods of H₂S from biogas based on physical, chemical, and biological approaches [5,6].

Biochar, derived from the pyrolysis of biomass, is a carbon material similar to an activated carbon. Biochar usually has a wide range of chemical compositions and surface properties depending on the biomass type, the heating rate, the residence time and the pyrolysis temperature [7]. Biochar is successfully utilized to mitigate climate change, improve soil fertility, and remove various contaminants in aqueous solutions as an alternative adsorbent, including heavy metals, excessive nutrients, and pharmaceuticals [8–12]. In comparison with an activated carbon, the manufacturing of biochar requires less energy and no pre- or post-activation processes, although it has a high adsorption ability and capacity [13]. Biochar is also the well-known means of carbon sequestration [14]. Thus, the objective of this work is to evaluate the potential of biochars derived from different types of biomass to eliminate H₂S and CO₂ from biogas.

2. Materials and Methods

2.1. Biochar Production and Characterization

Four types of optimized biochars derived from perilla leaf, soybean stover, Korean oak (*Quercus dentata*) and Japanese oak (also known as emperor oak) were used in this study. The powdered biomass of perilla leaf and soybean stover were pyrolyzed at 700 °C with a heating rate of 7 °C/min using a muffle furnace (N11/H Nabertherm, Lilienthal, Germany). A commercial biochar produced from Korean oak at 400 °C was purchased from the Gangwon Charmsoot Company located in Hoengseong-gun, Gangwon Province, Korea. The Japanese oak biochar produced at ~500 °C.

The physicochemical properties of all biochars were characterized, as shown in Table 1. The pH of each biochar was determined in a suspension of 1:5 (*w/v*) biochar:deionized water using a digital pH meter (Orion, Thermo Electron Corp., Waltham, MA, USA). Elemental composition (e.g., C, H, N, S, and O) of the biochars was determined by dry combustion, using an elemental analyzer (model EA1110, CE Instruments, Milan, Italy). Brunauer–Emmett–Teller (BET) specific surface area, total pore volume, and pore diameter of biochars were assessed using a gas sorption analyzer (NOVA-1200; Quantachrome Corp., Boynton Beach, FL, USA) and surface morphologies were also examined using a field emission scanning electron microscope (FE-SEM; 15.0 kv × 5.0 k) equipped with an energy dispersive spectrophotometer (SU8000, Hitachi, Tokyo, Japan). The content of moisture was determined by the weight loss after heating the biochars at 105 °C for 24 h to a constant weight. The content of mobile matter, reflecting the non-carbonized portion in biochar, was determined as the weight loss after heating in a covered crucible at 450 °C for 30 min. The ash content was determined as the residue remained after heating at 700 °C in an open-top crucible. The portion of biochar except ash is considered as fixed matter.

Table 1. Selected physicochemical characteristic of biochars.

Biochar	Moisture	Mobile Matter	Fixed Matter	Ash	pH [†]	C*	H*	O*	N*	S*	BET Surface Area	Pore Volume	Pore Size
					%						m ² /g	cm ³ /g	nm
Perilla	0.1	6.5	51.6	41.9	10.6	71.8	0.9	15.3	1.5	0.1	473.4	0.1	3.4
Korean oak	6.8	31.4	56.1	5.1	10.2	88.7	1.2	9.7	0.4	0.0	270.8	0.1	1.1
Japanese oak	1.5	31.3	63.9	3.3	9.9	89.9	2.4	7.5	0.2	0.0	475.6	0.2	1.1
Soybean stover ^a	0.4	14.7	67.8	17.2	11.3	81.9	1.4	15.5	1.3	0.0	420.3	0.2	1.1

[†] 1:5 biochar:water-ratio; * moisture and ash free basis; ^a values obtained from Ahmad et al. [8,9]; BET Surface Area = Brunauer–Emmett–Teller (BET) surface area.

2.2. Biogas Adsorption

The continuous adsorption experiments were performed using the subjected biochars. This experiment consisted of four major systems of fixed bed adsorber, mass flow controller, humidifier and biogas analyzer, as shown in Figure 1. A stream of simulated biogas containing gaseous mixtures of H₂S (0.3%), CO₂ (40%), and CH₄ (59.7%), under a relative humidity of 20% controlled by a water bath, was passed through a reactor for the simultaneous removal. The relative humidity was calculated by integrating the difference between the temperatures of water vapor in the water bath and the sorption column. A blank test was conducted to measure the feed concentration of biogas in a void system. For the single gas study, the concentration of each gas was fixed with N₂ as balance. The feed flow through the reactor was maintained at 300 mL/min. The temperature of a reaction was set to 50 °C. Then 0.5 g of biochar was placed in the center of the fixed-bed adsorber with the support of 0.1 g borosilicate glass fiber. The outlet concentration of the respective gases was recorded until the concentration of gases equaled the feed concentration. The inlet and outlet concentrations of gases were measured using a continuous gas analyzer system (MRU Vario Plus Industrial, Houston, TX, USA). The adsorbent bed height was about 8 mm. The adsorption capacity of biochars was expressed from adsorption breakthrough capacity at 5% from initial gas concentration and it was calculated according to the equation below:

$$q_t = \left(1 - \frac{C}{C_0}\right) \frac{Q_f t y_f}{m_c} \quad (1)$$

where q_t is the breakthrough sorption capacity at 5% from initial concentration; y_f is the mole fraction of the sorbate in the feed; Q_f is the volumetric feed flow rate at standard temperature and pressure (STP); C is the concentration of gas at time t ; C_0 is the initial feed concentration of gas and m_c is the mass of sorbent used inside the bed. The biochars were tested in two modes (i.e., single and simultaneous biogas gases). Each test was done in triplicate.

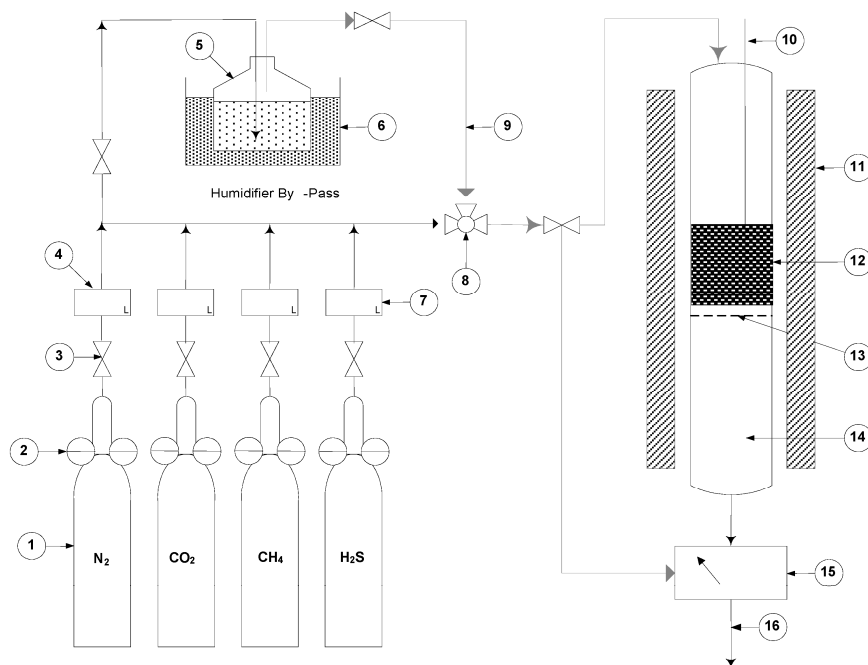


Figure 1. Schematic diagram of adsorption test rig. (1) Gas cylinders; (2) Pressure regulators; (3) Pinch valve; (4) Mass flow meter; (5) Humidifier; (6) Water bath; (7) Mass flow controller; (8) Three-way controller; (9) Insulated pipeline; (10) Thermocouple; (11) Furnace; (12) Biochar; (13) Glass wool; (14) Reactor; (15) Flue gas analyzer; (16) Vent.

3. Results and Discussion

3.1. Characterization of Biochars

The physicochemical characteristics of the four different biochars used in this study are shown in Table 1. All biochars were alkaline (pH 9.9–11.3) with a typical pH range of common biochars produced at high temperatures [15,16]. The Brunauer–Emmett–Teller (BET) surface areas of the Japanese oak and perilla biochars showed a similarity ($\sim 470 \text{ m}^2/\text{g}$) and the lowest BET surface area of $270.8 \text{ m}^2/\text{g}$ was observed for Korean oak biochar derived from pyrolysis at a relatively low temperature compared to the Japanese oak and perilla biochars. The average pore diameters of all biochars were less than 2 nm, assumed in a range of micropores. The scanning electron micrographs (SEM) images of perilla biochar show the presence of micropores (Figure 2). These images are similar to those in a study of Ahmad et al., which showed the SEM images of soybean stover biochar produced from the same condition of pyrolysis [9]. The Japanese and Korean oak biochars had less ash contents (3.3% and 5.1%, respectively) than the soybean stover and perilla biochars (17.2% and 41.9%, respectively). The relatively high ash contents in the soybean stover and perilla biochars may be due to leafy feedstock. The carbon contents of the Japanese and Korean oak biochars showed higher values than those of the soybean stover and perilla biochars.

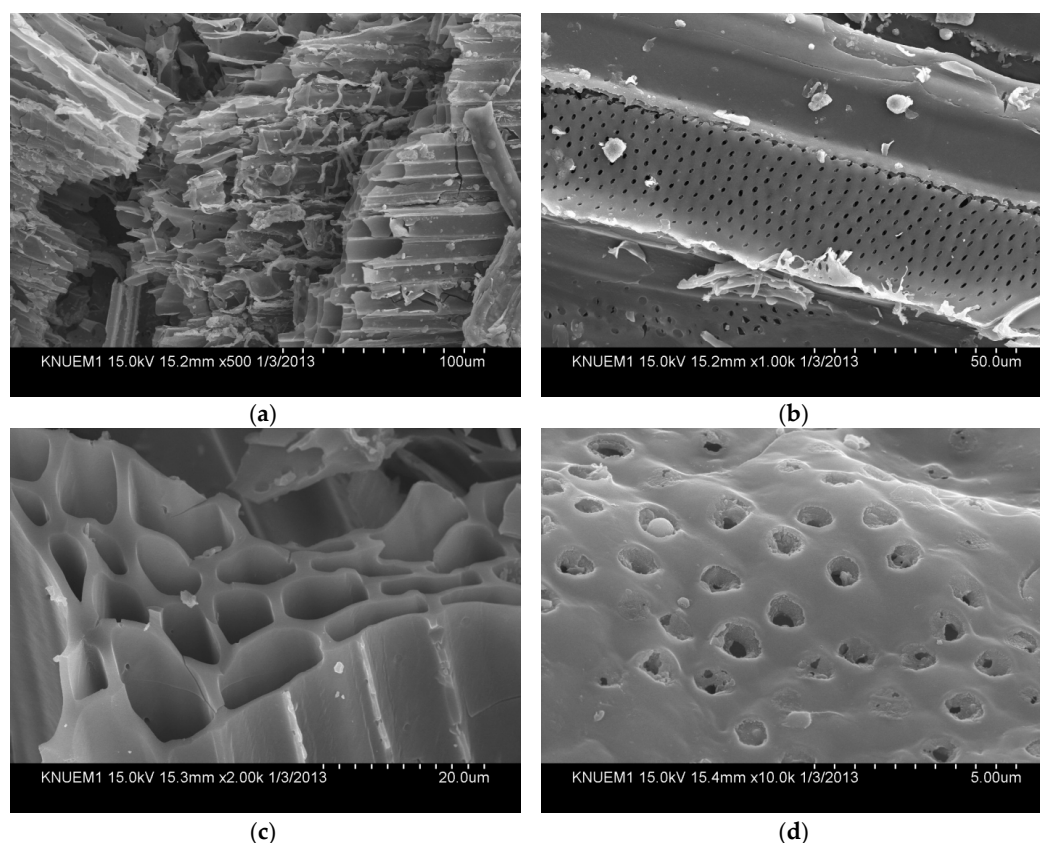


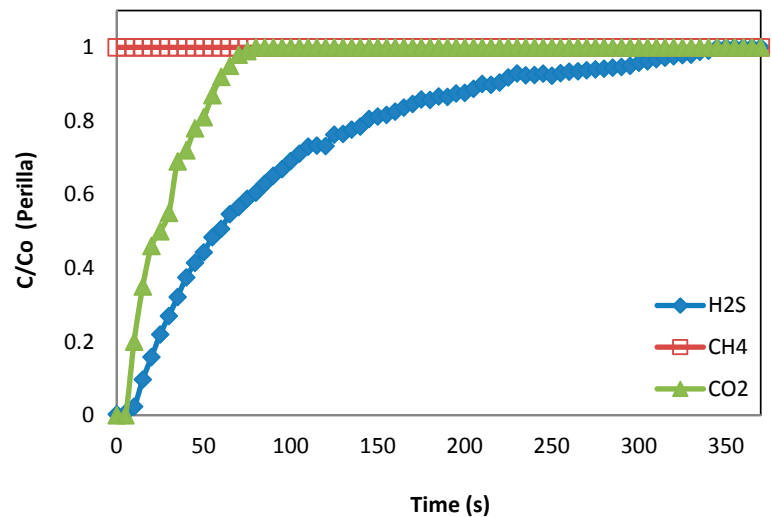
Figure 2. Scanning electron micrographs (SEM) of perilla biochar at different magnification scales: (a) $\times 500$; (b) $\times 1000$; (c) $\times 2000$; (d) $\times 10000$ magnification.

3.2. Breakthrough Capacity

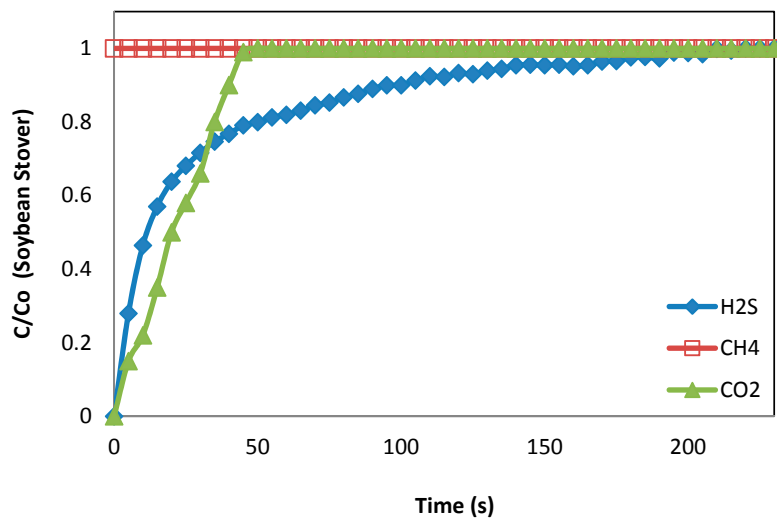
The breakthrough curves and capacities for the four different biochars are shown in Figure 3 and Table 2. The C/C_0 versus time figure was plotted based on the average value of three repetition of the adsorption study for each biochar. The significant error was less than 4% for each data point. The breakthrough curves were plotted based on the adsorption rate of each biochar for the simulated

biogas composition. The breakthrough capacities of all biochars clearly showed no capacity to adsorb CH_4 gas. This is advantageous for biogas purification as CH_4 must be retained for enhancing the biogas capacity for energy harvesting.

The biochars may not be an adsorbent of CH_4 because of their pore sizes. Adinata et al. [17] reported that only molecular-sized carbons in the range of 0.33 to 0.40 nm are capable of separating CH_4 from CO_2 . The pore sizes of the subjected biochars were bigger than 1.0 nm, and therefore CH_4 managed to escape without being adsorbed by the biochars. It could also be due to the competition between H_2S and CO_2 , which have smaller molecular sizes than CH_4 .



(a)



(b)

Figure 3. Cont.

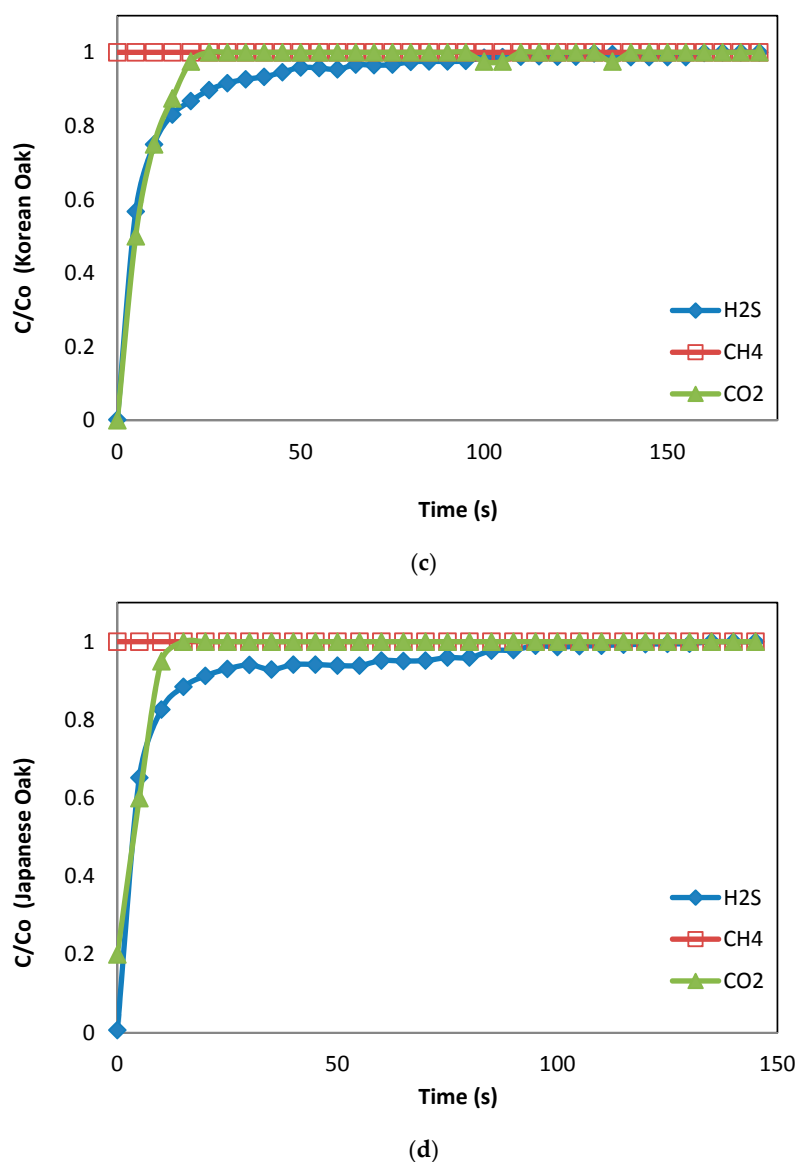


Figure 3. Breakthrough curves of simultaneous removal of H₂S, CH₄, and CO₂ on different biochars: (a) perilla; (b) soybean stover; (c) Korean oak; and (d) Japanese oak.

Table 2. Adsorption capacity of biochar during simultaneous and single-gas presentation.

Biochar	Adsorption Capacity (mmol/g)					
	Simultaneous			Single		
	H ₂ S	CO ₂	CH ₄	H ₂ S	CO ₂	CH ₄
Perilla	0.208	0.126	0.000	0.537	2.312	0.099
Korean oak	0.022	0.027	0.000	0.178	0.597	0.092
Japanese oak	0.018	0.012	0.000	0.167	0.379	0.064
Soybean stover	0.072	0.082	0.000	0.308	0.707	0.094

The breakthrough times of H₂S and CO₂ indicated that they were adsorbed. The breakthrough times for the Japanese and Korean oak biochars were shorter and steeper than those of the perilla and soybean stover biochars. This means that Japanese and Korean oak biochars adsorb H₂S and CO₂; however, the sorption capacities can be poor compared to perilla and soybean stover biochars.

Perilla and soybean stover biochars showed longer breakthrough times, indicating better retention of H₂S and CO₂ adsorbate (Figure 3). Shang et al. [18] stated that the H₂S breakthrough capacity is also governed by the local pH within the pore system.

It is noted that Japanese oak biochar had the lowest pH and shortest breakthrough time compared to other biochars in this study; however, this trend is quite similar to Korean oak biochar with a similar pH value. Thus, the Japanese oak biochar may suppress the dissociation of H₂S and indirectly limit the sulfur oxidation even though the Japanese oak biochar has a high BET surface area. The perilla biochar shows better retention of H₂S than the soybean stover biochar. The perilla biochar recorded the highest BET surface area among the subjected biochars, indirectly suggesting that the H₂S breakthrough capacity is not only governed by pH but also by the pore system in the biochar. Similarly, the influence of the pore structure and BET surface area on the adsorption of H₂S was reported by Gutiérrez Ortiz et al. [6], who used the sewage sludge char. In this study, the H₂S adsorption capacity of the subjected biochars was perilla > soybean stover > Korean oak > Japanese oak.

Figure 3 shows that all the subjected biochars adsorbed CO₂. The patterns of biochars for CO₂ adsorption capacity were similar to H₂S, but the adsorption capacity was much lower (Table 2); the breakthrough curve for CO₂ in Figure 3 was very steep. Creamer et al. [14] suggested that the adsorption of CO₂ onto biochar was mainly controlled by physisorption, which is a weak interaction raised from intermolecular forces (e.g., van der Waals forces).

This signifies that the biochars with a large BET surface area show a better adsorption ability than those with a small BET surface area. This was further proven by the perilla biochar showing a higher capacity compared to the others. Besides, Zhang et al. [19] revealed that the presence of nitrogenous groups tends to increase the CO₂ adsorption capacity in an activated carbon.

Table 1 shows that the presence of N groups in the perilla and soybean stover biochars was higher compared to those of the Japanese and Korean oak biochars. This finding supports that the perilla biochar has a better capacity for CO₂ adsorption than the other biochars. The CO₂ adsorption capacities of biochars were positively correlated with the N contents of the biochars ($R^2 = 0.871$), suggesting their interdependence and the importance of N groups for CO₂ sorption. The strong interaction between the acidic CO₂ and the basic nitrogenous functional groups of biochars may promote the physisorption of CO₂ on biochar surfaces [14].

It is noticed that the adsorption of H₂S was more complete than that of CO₂ (Figure 3). A recent study using sugarcane bagasse biochar showed that it is a promising CO₂-adsorbing material with capacity of about 70 mg/g [14]. However, the current study shows a much lower capacity (16 mg/g). The decrease in the adsorption capacity could be due to competition for the sorption sites between CO₂ and H₂S and the starting material used to produce the biochars. This study measurement was taken during simultaneous exposure to both CO₂ and H₂S, whereas the report by Creamer et al. [14] was conducted using only CO₂. In order to prove the competition, a single-gas adsorption study for CO₂, CH₄, and H₂S was performed. Figures 4–6 show the breakthrough curves for the single-gas study. Figure 4 proves that without the presence of CH₄ and CO₂, all four biochars showed a longer H₂S adsorption breakthrough time compared to the simultaneous study. A similar trend was seen for the other gases as well, in Figures 5 and 6, without the presence of other gases. A single-gas adsorption (CO₂) by the perilla yield achieved about a 294 mg/g adsorption capacity compared to only 70 mg/g by Creamer et al. [14]. A comparable work using activated carbon also reported that the presence of CO₂ inhibited H₂S adsorption due to the competitive adsorption and reaction between CO₂ and H₂S on the surface of the activated carbon [20]. The saturation time for H₂S and CO₂ in the single runs was longer than in the simultaneous run. In terms of the preference of adsorption, all biochars showed a longer breakthrough time for H₂S than for CO₂. This is because the adsorption of CO₂ was mainly through physisorption, whereas for H₂S, the adsorption may be governed by both physisorption and the local pH within the pores. For CH₄ gas (Figure 6) it was observed that the breakthrough time was very short (less than 70 s). This shows that the biochars could hardly adsorb CH₄, even without

any competition with other gases, and manifested in the simultaneous adsorption with CO₂ and H₂S. Arami-Niya et al. [21] stated that only narrow, microporous-sized particles can adsorb methane.

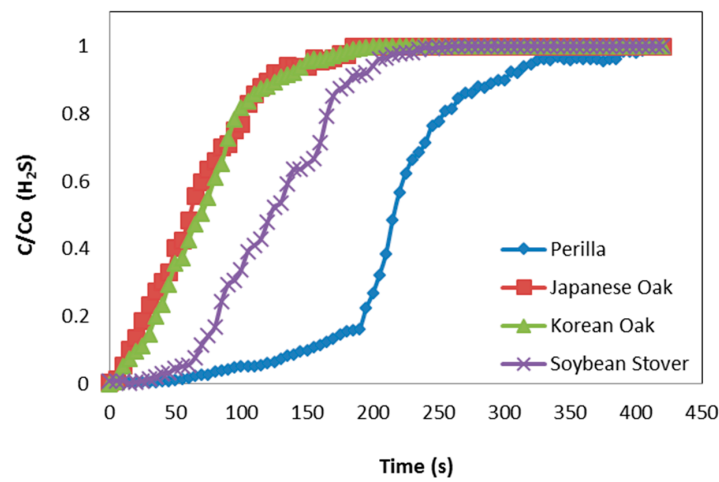


Figure 4. Breakthrough curves of single H₂S sorption on different biochars.

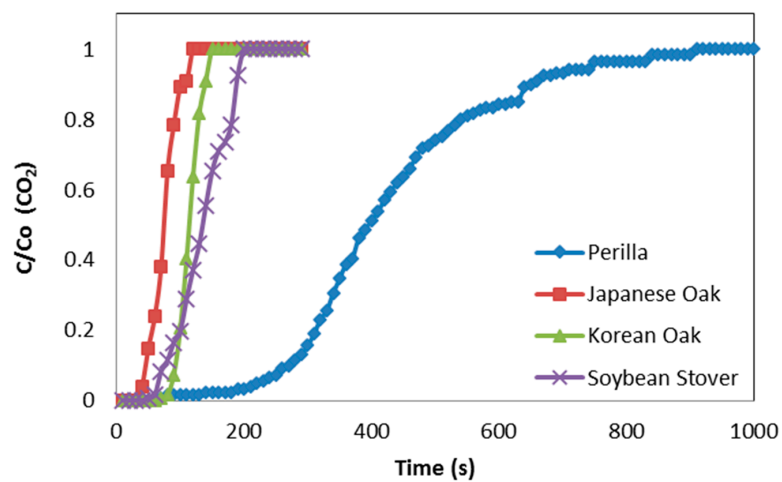


Figure 5. Breakthrough curves of single CO₂ sorption on different biochars.

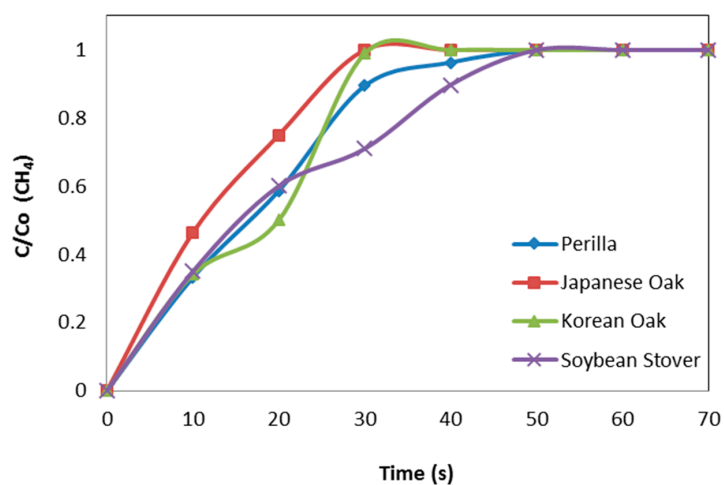


Figure 6. Breakthrough curves of single CH₄ sorption on different biochars.

4. Conclusions

Biochars derived from perilla, Japanese and Korean oaks, and soybean stover were shown to be promising scrubbing adsorbents for biogas. The highest breakthrough capacities and removal rates of the biogases H₂S and CO₂ were reported by perilla biochar followed by soybean stover biochar, before Korean oak and Japanese oak biochars, respectively. Simultaneous removal shows the competition of sorption sites by H₂S and CO₂ on the biochars. The results suggest that H₂S adsorption was more preferred than CO₂, due to the physical and chemical properties of the biochars. Biochars are a sustainable, low-cost material as the feedstock can be made from renewable and waste biomass materials.

Acknowledgments: This research is supported by 2015 Research Grant from Kangwon National University (No. 520160387) and the Korea Ministry of Environment, as a Geo-Advanced Innovative Action Project (G112-00056-0004-0). Instrumental analyses were supported by the Korea Basic Science Institute, the Environmental Research Institute, and the Central Laboratory of Kangwon National University, Korea. The study was also partly supported by Long-Term Research Grant Scheme (1216135615) from Universiti Sains Malaysia.

Author Contributions: Sumathi Sethupathi, Ming Zhang and Anushka Upamali Rajapaksha conducted the experiment and wrote the manuscript. Sang Ryong Lee, Norhusna Mohamad Nor, and Abdul Rahman Mohamed contributed to the data analysis. Mohammad Al-wabel, and Sang Soo Lee contributed to language editing and manuscript modifications. Yong Sik Ok is the principal investigator and designed the experiment. All authors have read and approved the final manuscript.

Conflicts of Interest: The authors declare no conflict of interest.

References

- Ohimain, E.I.; Izah, S.C. A review of biogas production from palm oil mill effluents using different configurations of bioreactors. *Renew. Sustain. Energy Rev.* **2017**, *70*, 242–253. [[CrossRef](#)]
- Ji, C.M.; Eong, P.P.; Tia, T.B.; Seng, C.E.; Ling, C.K. Biogas from palm oil mill effluent (POME): Opportunities and challenges from Malaysia's perspective. *Renew. Sustain. Energy Rev.* **2013**, *26*, 717–726.
- Hosseini, S.E.; Wahid, M.A. Utilization of biogas released from palm oil mill effluent for power generation using self-preheated reactor. *Energy Convers. Manag.* **2015**, *105*, 957–966. [[CrossRef](#)]
- Taliwa, Y.; Matsumoto, T.; Oshita, K.; Takaoka, M.; Morisawa, S.; Takeda, N. Characterization of trace constituents in landfill gas and a comparison of sites in Asia. *J. Mater. Cycles Waste Manag.* **2009**, *11*, 305–311.
- Ho, K.L.; Chung, Y.C.; Lin, Y.H.; Tseng, C.P. Microbial populations analysis and field application of biofilter for the removal of volatile-sulfur compounds from swine wastewater treatment system. *J. Hazard. Mater.* **2008**, *152*, 580–588. [[CrossRef](#)] [[PubMed](#)]
- Gutiérrez Ortiz, F.J.; Aguilera, P.G.; Ollero, P. Biogas desulfurization by adsorption on thermally treated sewage-sludge. *Sep. Purif. Technol.* **2014**, *123*, 200–213. [[CrossRef](#)]
- Ahmad, M.; Rajapaksha, A.U.; Lim, J.E.; Zhang, M.; Bolan, N.; Mohan, D.; Vithanage, M.; Lee, S.S.; Ok, Y.S. Biochar as a sorbent for contaminant management in soil and water: A review. *Chemosphere* **2014**, *99*, 19–33. [[CrossRef](#)] [[PubMed](#)]
- Ahmad, M.; Lee, S.; Oh, S.E.; Mohan, D.; Moon, D.; Lee, Y.; Ok, Y.S. Modeling adsorption kinetics of trichloroethylene onto biochars derived from soybean stover and peanut shell wastes. *Environ. Sci. Pollut. Res.* **2013**, *20*, 8364–8373. [[CrossRef](#)] [[PubMed](#)]
- Ahmad, M.; Lee, S.S.; Rajapaksha, A.U.; Vithanage, M.; Zhang, M.; Cho, J.S.; Lee, S.E.; Ok, Y.S. Trichloroethylene adsorption by pine needle biochars produced at various pyrolysis temperatures. *Bioresour. Technol.* **2013**, *143*, 615–622. [[CrossRef](#)] [[PubMed](#)]
- Awad, Y.M.; Blagodatskaya, E.; Ok, Y.S.; Kuzyakov, Y. Effects of polyacrylamide, biopolymer and biochar on the decomposition of ¹⁴C-labeled maize residues and on their stabilization in soil aggregates. *Eur. J. Soil Sci.* **2013**, *64*, 488–499. [[CrossRef](#)]
- Vithanage, M.; Rajapaksha, A.U.; Tang, X.; Thiele-Bruhn, S.; Kim, K.H.; Lee, S.E.; Ok, Y.S. Sorption and transport of sulfamethazine in agricultural soils amended with invasive-plant-derived biochar. *J. Environ. Manag.* **2014**, *141*, 95–103. [[CrossRef](#)] [[PubMed](#)]
- Kong, Z.; Liaw, S.B.; Gao, X.; Yu, Y.; Wu, H. Leaching characteristics of inherent inorganic nutrients in biochars from the slow and fast pyrolysis of mallee biomass. *Fuel* **2014**, *128*, 433–441. [[CrossRef](#)]

13. Sun, Y.; Gao, B.; Yao, Y.; Fang, J.; Zhang, M.; Zhou, Y.; Chen, H.; Yang, L. Effects of feedstock type, production method, and pyrolysis temperature on biochar and hydrochar properties. *Chem. Eng. J.* **2014**, *240*, 574–578. [[CrossRef](#)]
14. Creamer, A.E.; Gao, B.; Zhang, M. Carbon dioxide capture using biochar produced from sugarcane bagasse and hickory wood. *Chem. Eng. J.* **2014**, *249*, 174–179. [[CrossRef](#)]
15. Lehmann, J.; Joseph, S. *Biochar for Environmental Management: Science and Technology*; Earthscan: London, UK; Sterling, VA, USA, 2009.
16. Park, J.H.; Ok, Y.S.; Kim, S.H.; Kang, S.W.; Cho, J.S.; Heo, J.S.; Dalaune, R.D.; Seo, D.C. Characteristics of biochars derived from fruit tree pruning wastes and their effects on lead adsorption. *J. Korean Soc. Appl. Biol. Chem.* **2015**, *58*, 751–760. [[CrossRef](#)]
17. Adinata, D.; Daud, W.M.A.W.; Aroua, M.K. Production of carbon molecular sieves from palm shell based activated carbon by pore sizes modification with benzene for methane selective separation. *Fuel Process. Technol.* **2007**, *88*, 599–605. [[CrossRef](#)]
18. Shang, G.; Shen, G.; Liu, L.; Chen, Q.; Xu, Z. Kinetics and mechanisms of hydrogen sulfide adsorption by biochars. *Bioresour. Technol.* **2013**, *133*, 495–499. [[CrossRef](#)] [[PubMed](#)]
19. Zhang, C.; Song, W.; Sun, G.; Xie, L.; Wang, J.; Li, K.; Sun, C.; Liu, H.; Snape, C.E.; Drage, T. CO₂ capture with activated carbon grafted by nitrogenous functional groups. *Energy Fuel* **2013**, *27*, 4818–4823. [[CrossRef](#)]
20. Sitthikhankaew, R.; Chadwick, D.; Assabumrungrat, S.; Laosiripojana, N. Effects of humidity, O₂, and CO₂ on H₂S adsorption onto upgraded and KOH impregnated activated carbons. *Fuel Process. Technol.* **2014**, *124*, 249–257. [[CrossRef](#)]
21. Arami-Niya, A.; Daud, W.M.A.W.; Mjalli, F.S. Comparative study of the textural characteristics of oil palm shell activated carbon produced by chemical and physical activation for methane adsorption. *Chem. Eng. Res. Des.* **2010**, *89*, 657–664. [[CrossRef](#)]



© 2017 by the authors; licensee MDPI, Basel, Switzerland. This article is an open access article distributed under the terms and conditions of the Creative Commons Attribution (CC-BY) license (<http://creativecommons.org/licenses/by/4.0/>).